Atomic structure of Si{001}2×1

W. S. Yang* and F. Jona
Department of Materials Science and Engineering, State University of New York, Stony Brook, New York 11794

P. M. Marcus
IBM Research Center, Yorktown Heights, New York 10598

(Received 4 March 1983)

New experiments on reconstructed Si{001}2×1 and their analysis by low-energy electron diffraction (LEED) are reported. A new structural model containing asymmetric and buckled dimers and strains extending to three and four atomic layers is presented, which fits the LEED data substantially better than any other model tested. The new structure involves a dimer length of 2.54 Å, an average contraction of first-layer spacing of 8%, and three asymmetric displacements of the dimer atoms. A detailed discussion of the needed intensity-averaging procedures among eight equivalent domains is presented. Two theoretical structural models for Si{001}2×1 developed by others on the basis of minimization of total energy are shown to fail the LEED test.

I. INTRODUCTION

The Si{001}2×1 surface structure is remarkable in two respects: (1) the reconstruction to a 2×1 surface cell involves large movements of the surface atoms which have been attributed to the formation of a new surface bond from dangling bonds on adjacent Si atoms, the so-called "surface dimer"; (2) the strain produced by this new bond then spreads through some five atomic layers of the crystal, as pointed out by Appelbaum and Hamann.[1,2] The many theoretical[1,2] and experimental[3–10] techniques applied to study the surface in recent years have all made use of dimerized structures with various types and amounts of asymmetry. However, a structure should not be called established until the low-energy electron diffraction (LEED) test is satisfied, i.e., until it gives calculated LEED spectra in satisfactory quantitative correspondence with the observed LEED spectra. The purpose of the present work is to present a structural model for Si{001}2×1 which passes the LEED test,[11] to show that all previously proposed structures do not pass the LEED test, and to make the point that the LEED test was essential in arriving at the correct structural model.

We believe that the determination of this surface structure with its many parameters and deep strains could only be carried out at this time by LEED intensity analysis. We wish to emphasize that LEED intensity analysis is a powerful and reliable technique for determining surface structure when carried out with a large data base and both visual and objective (r factor) evaluation of goodness of fit of theory to experiment as in the present work. The technique is powerful because with a large data base it uses hundreds of independent pieces of information to fix a much smaller number of parameters, and is independent of the poorly known electronic state of the system studied, i.e., the nature of the binding; it is reliable because it rests on a few simple well-tested assumptions about the elastic coherent scattering of electrons in crystals at energies well above the binding energies, which have led to numerous very-high-quality fits of theory to experiment in simple well-defined structures.[12] In sum, a structure that passes the LEED test when carried out as described above is not merely a plausible model dependent on a variety of uncontrolled approximations and assumptions but a direct fitting of experiment on such a scale and with such established measures of goodness of fit as to make it very unlikely that the result is a mere coincidence. What cannot be assured in LEED crystallography, since the analysis is based on trial and error, is that it will succeed in finding the correct structure, especially in complicated cases with many parameters, since the procedure for deducing the parameters from the data is not systematic; success depends on clues that provide a reasonable starting point for trial and correction. We note that for Si{001}2×1 with two atoms per layer and five layers, there are 30 structural parameters in a full definition of the structure and the testing of even one set of values requires lengthy calculation.

The present work on Si{001}2×1 used special procedures to deal with these difficulties: (1) The overall computational load was reduced by use of a quasidynamical procedure in the early stages of surveying and rejecting structures; this procedure gains computer time by neglecting all multiple scattering in each layer and is not too bad for a scatterer that is only moderately strong like Si. The final stages, however, involved full dynamical calculations. (2) The experimental intensity data were collected after deposition on the surface of small amounts of metallic impurities which are believed to reduce the coverage by 2×2 and $c(2\times4)$ reconstructions. (3) The length of the search process for best-fit parameters was reduced by use of initial deep-strain values as suggested by the works of Appelbaum and Hamann[1,2] and of Tong and Maldonado,[3] and further reduced by the use of a statistical method, the method of orthogonal experimental design, that selects a small number of sets of trial values of parameters around the initial guess to estimate a better set.

The structure that has emerged from the fitting process produces an r factor which past experience tells us is characteristic of a reliable structure, and shows to the eye a fairly satisfactory fit of theory to experiment. The fit is

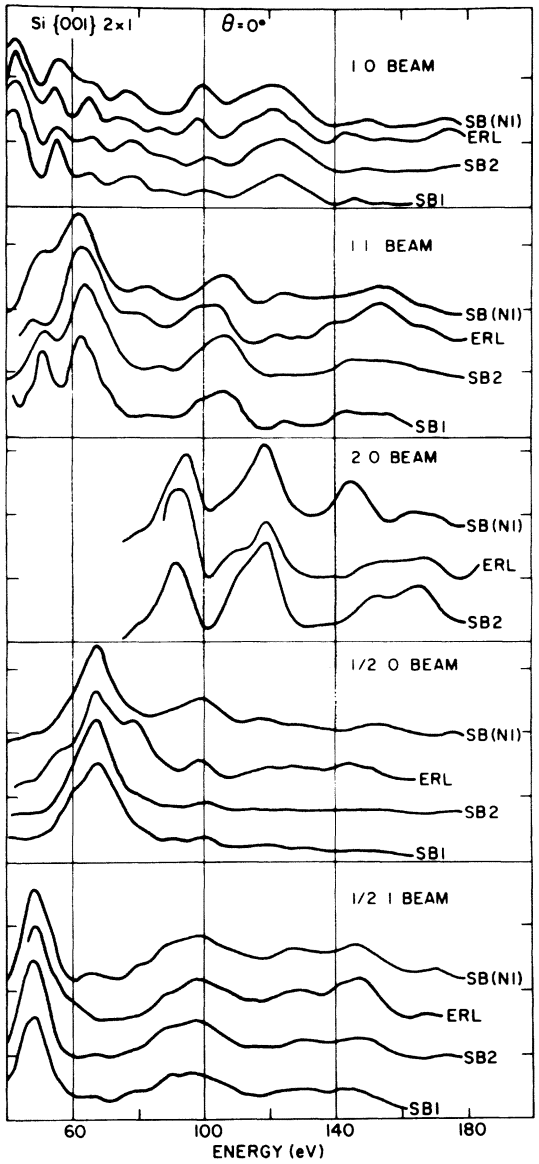

FIG. 1. Experimental LEED spectra from Si{001}2×1 at normal incidence from different sources. SB(NI): nickel-stabilized structure (this work). ERL: Erlangen data (Ref. 16). SB2: ion-bombarded and annealed surface (this work). SB1: ion-bombarded and annealed surface (SB data in Ref. 13).

much better than any other structure we have tried, and was not easily achieved, but is the end product of a lengthy search. We believe that such a fit is very unlikely to be a chance coincidence. If correct, this structure has important implications for the validity of both local-density, pseudopotential slab calculations (which give much shorter dimer bonds) and the best cluster calculation with detailed allowance for correlation between electrons (which gives no buckling).

II. EXPERIMENTAL

Several sets of LEED intensity spectra were already in existence at the beginning of the present study. Three such sets were compared to one another in 1977 in a joint publication by three laboratories[13] (Stony Brook, Milwaukee, and Warwick, referred to as SB1, *M* and *W*, respectively) where the conclusion was reached that, with the exception of the $\frac{3}{2}$ 1 (and possibly the 2 0) beam at normal electron incidence, the agreement between sets was satisfactory. Although no visible evidence for structures other than the 2×1 was reported by any of the three laboratories in their observations of LEED patterns, we decided to repeat the experiment once again in order to test the effect of different surface-preparation procedures upon the shape of LEED intensity spectra. This task was made easier by the use of a data-acquisition system consisting of a television camera, video monitor, and microcomputer that allows rapid recording and plotting of the intensity spectra.

The experiment involved cleaning several samples of Si{001} in a display-type LEED chamber, the cleaning procedure consisting of sequences of argon-ion bombardments (argon pressures around 5×10^{-5} Torr, ion energies 350–400 eV, ion currents 3–3.5 μA) followed by 30-sec anneals at temperatures as high as 1200 °C. The LEED patterns observed after these treatments were always characteristic of a mixture of equal amounts of 2×1 and 1×2 domains with no visible evidence for other structures. These observations are, of course, in contrast to those of a few other workers[8,14,15] who observed diffracted beams from a $c(4\times2)$ structure. More recently, Mueller *et al.*[16] observed diffraction features from five structures: 2×1, $c(4\times2)$, $c(4\times4)$, $c(8\times8)$, and 2×8, the concentration of each depending on the annealing temperature and cooling rate, and all believed to be characteristic of a clean surface. The LEED intensity spectra measured from our surfaces in the present work were reproducible—they are compared with our own 1977 data and with others in Fig. 1. We used two samples with different resistivities (9×10^{-3} and 2000 Ω cm) and found no differences between corresponding LEED spectra.

Experiments involving deposition of metals on a clean Si{001}2×1 surface revealed an interesting phenomenon. After only a few seconds of exposure of the surface, at room temperature, to a vapor of Ni, Pd, or Pt produced by a hot filament, the 2×1 LEED pattern appeared markedly enhanced in brightness and contrast—the LEED spots seemed sharper and the background more uniformly lower. Auger-electron spectroscopy of the surface at this stage revealed no Auger line characteristic of the deposited metal above the noise. When the exposure of the surface to the metal vapor was prolonged to achieve an estimated coverage of two or more monolayers, the background in the LEED pattern increased visibly, but flashing the sample to about 1300 °C regenerated a sharp, low-background LEED pattern. Under these conditions, the Auger lines of the deposited metals were mostly undetectable. A reliable measurement of the amount of metallic impurity still present on the Si surface was impossible. Experience with other adsorbates allowed us only to estimate that the surface coverage was probably less than 5% of a monolayer. We hypothesized that the Ni, Pd, or Pt impurities played the role of stabilizers of the 2×1 structure, favoring the growth of 2×1 and 1×2 domains at the expense of other reconstructions or disorder. The LEED spectra measured after this hypothetical stabilization of the 2×1 structure were similar but not identical to

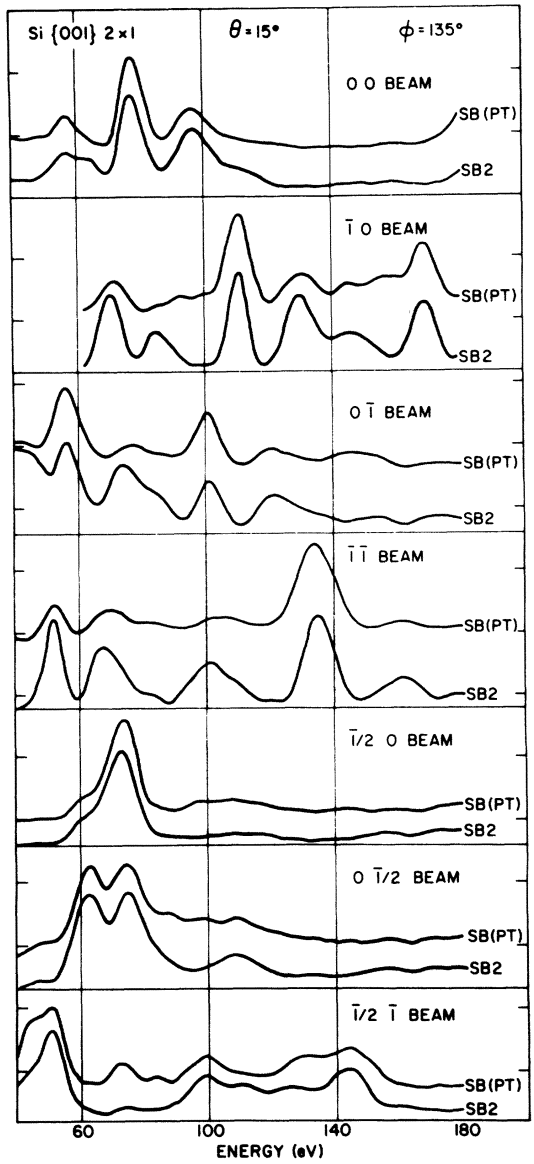

FIG. 2. Experimental LEED spectra from Si{001}2×1 at $\theta=15°$, $\phi=135°$ from two sources. SB(PT): platinum-stabilized structure. SB2: ion-bombarded and annealed structure.

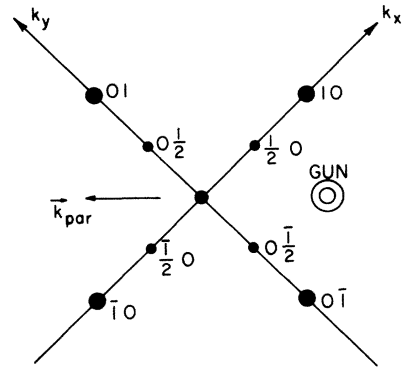

FIG. 3. Schematic LEED pattern from Si{001}2×1 showing the orientation of component $\vec{k}_{par}$ parallel to the surface of incident $\vec{k}$ vector, and position of the gun in conventional display-type LEED apparatus.

those from the unstabilized surface. The spectra from Ni-, Pd-, or Pt-stabilized surfaces were not identical to one another either, although in general the differences among them were smaller than between them and those from the unstabilized surface.

Figure 1 allows the comparison of normal-incidence spectra from different surfaces, namely: (1) a Ni-stabilized surface as described above [denoted SB(NI)]; (2) a heat-treated clean surface as described by Mueller *et al.*[16] (denoted ERL for Erlangen); (3) an ion-bombarded and annealed clean surface as described above (denoted SB2); (4) a (similarly treated) surface used in the 1977 experiment[13] (denoted SB1). The ERL, SB2, and SB1 spectra have been translated along the abscissa axis by amounts varying between 0 and 4 eV in order to match high-energy peaks or, failing those, the most pronounced peaks to one another. Such shifts imply only uncertainties in the inner potential but make it easier to recognize differences among spectra from different sources. It is impossible, at this time, to decide whether the differences are indeed a consequence of small but varying surface coverage by structures other than the 2×1, or merely fluctuations caused by experimental errors. Such detailed comparison between LEED spectra for the same surface from different sources has never been done in recent years, not even for surfaces known to have only one structure,[17] and there is therefore no experience on which to base a judgment. Nevertheless, we will assume that most of the differences detected in Fig. 1 are caused by the coexistence with 2×1 of other structures. The data believed to be representative of the "purest" 2×1 are the top two curves in each panel in Fig. 1. It may be interesting to note that where these curves differ most from one another (2 0 beam), agreement with the model developed in this work and discussed below is at its worst. The next largest difference is exhibited by the $\frac{1}{2}$ 0 beam: In this case the model presented below agrees better with the ERL curve at low energies and with the SB2 curve at high energies. Figure 2 compares experimental LEED spectra at non-normal incidence. In this case only two curves are available for each beam: the impurity-stabilized (in the figure, Pt-stabilized) and the clean data collected in this work (SB2).

The analysis described below was limited to the impurity-stabilized data, in particular: seven spectra at normal incidence (1 0, 1 1, 2 0, $\frac{1}{2}$ 0, $\frac{1}{2}$ 1, $\frac{3}{2}$ 0, $\frac{3}{2}$ 1) and seven at $\theta=15°$, $\phi=135°$ (0 0, $\bar{1}$ 0, 0 $\bar{1}$, $\bar{1}\,\bar{1}$, $\frac{1}{2}$ 0, 0 $\frac{\bar{1}}{2}$, $\frac{1}{2}\,\bar{1}$). A schematic LEED spectrum as observed on the fluorescent screen of a conventional LEED apparatus is depicted in Fig. 3. The direction of $\vec{k}_{par}$ (component of incident $\vec{k}$ parallel to the surface) and the location of the LEED gun are also indicated. The values of θ and ϕ quoted above follow the convention described elsewhere (see e.g., Jona[18]).

III. CALCULATIONS AND ANALYSIS

The LEED intensity calculations were done with two different computer programs in the course of the analysis. In the initial stages, the time-saving quasidynamical (QD) program[19] that was developed after the scheme of Tong

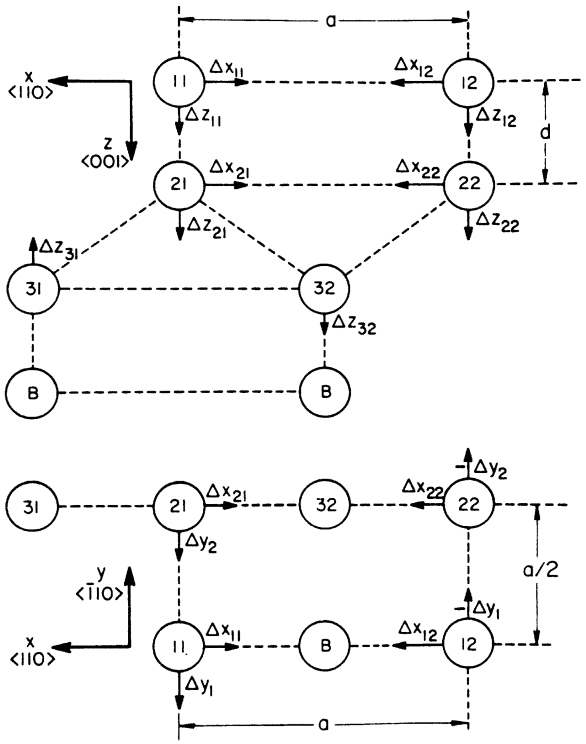

FIG. 4. Schematic, three-layer distorted, asymmetric, and buckled dimer model for Si{001}2×1. The upper drawing represents a projection on a {110} plane (side view), the lower drawing represents a projection on a {001} plane (top view). 11 and 12 are first-layer atoms; 21 and 22 are second-layer atoms; 31 and 32 are third-layer atoms; B are the bulk atoms. The arrows indicate displacements from bulk equilibrium positions leading to the 2×1 reconstruction. Magnitudes of the displacements are given in Table I for several models: $a=3.84$ Å; $d=1.36$ Å.

et al.[20] was used to explore a large number of variations of the buckled asymmetric dimer model. In the later stages, the full-dynamical (FD) CHANGE program was used that is described elsewhere.[21] The electron wave function was approximated with 58 beams and 5 phase shifts. The Si potential was the same as that used in the analysis[21] of impurity-stabilized Si{111}1×1. The inner potential was chosen initially as $V_0=-(7+3.5i)$ eV, both the real and the imaginary part being adjustable parameters in the theory-experiment fitting process; the final value was $V_0=-(9+3.5i)$ eV. The root-mean-square amplitude of atomic vibrations was $\langle u^2\rangle^{1/2}=0.101$ Å.

The starting point of the analysis was the type of model involving asymmetric and buckled dimers that had emerged from earlier LEED studies of both Si{001} and Ge{001}.[19,22] In those studies the best models of that type that were tested represented considerable improvement over previous attempts, but the agreement between theory and experiment was still considered too rudimentary to justify the claim to a satisfactory solution. The *r*-factor[23] values varied at normal incidence from 0.18 to 0.55, depending on the LEED spectrum considered, and were particularly large at non-normal incidence, between 0.3 and 0.9, indicating low to no reliability of the structural models tested. (We recall that values of the *r* factor used in our studies up to 0.20—0.25 signify excellent to good agreement, values above 0.3, mediocre, and above 0.4, poor to no agreement between theory and experiment.[23]) In the early stages of the present analysis, the QD program was used because of its economy in computer time. Several parameters were varied, all involving distortions of the bulk structure in the top 4—5 atomic layers, and the correspondence with experiment was evaluated visually rather than by the *r* factor. At this stage the analysis was limited to normal-incidence data. Progress was slow because the number of structural parameters was very large by present-day LEED standards—in a five-layer model, with two atoms per layer there are in principle 30 parameters to determine. Even in a simplified three-layer model, such as that depicted in Fig. 4 and ultimately adopted for the FD calculations, there are 12 structural parameters to refine. We note that this problem is orders of magnitude more complex than any other quantitative LEED structure analysis done to date. There are no established rules or procedures about how to approach the solution of a problem of this magnitude. By trial and error we succeeded in improving the visual fit to the normal-incidence data to some extent. We then tried the method of orthogonal experimental design (OED),[24] a method aimed at limiting the numbers of calculations needed in order to find the extrema of a function. In our case the function is the mean *r* factor for the data at normal incidence. The number of calculations needed to minimize the *r* factor depends, of course, on the number of parameters to be optimized and the number of values that each parameter is allowed to take. For example, with 13 parameters (namely, the 12 structural parameters defined in Fig. 4 plus the imaginary part of the potential), each varied over three values, the OED method prescribes only a subset of 27 calculations to estimate an improved set of 13 values. For these calculations we used the CHANGE program and for the measure of fit to experiment we used exclusively the *r* factor.[23] We then took the "best" model produced by the OED method and made small adjustments of some of the parameter values by using both the *r* factor and the visual comparison of corresponding spectra as measures of fit. The final model, called SICM33 and considered the most reliable for producing the best overall agreement between theory and experiment, is defined in terms of 12 parameter values in Table I. We postpone the description and the discussion of this model to Sec. IV in order to explain here the averaging procedures that are needed in order to compare the calculated LEED spectra to the observed ones.

In LEED crystallography the intensity calculations are done for a specific distortion of the surface structure with respect to the bulk structure. In some cases, however (the present being one of them), there are a number of equivalent ways of producing the distortion, and the surface may contain different regions or domains with different orientations of the same structure. It becomes necessary then to average the intensities produced by all domains present on the surface before comparing the calculated LEED spectra to the observed LEED spectra. In general, the assumption is made that all possible domains are present in equal concentrations on the surface. Discussions about how to do the averaging among domains

TABLE I. Structural parameter values for Si{001}2×1 models. Each number in the table represents the value (in Å) of the corresponding atomic shift along the axes shown in Fig. 4.

Model	Δx_{11}	Δy_1	Δz_{11}	Δx_{12}	Δz_{12}	Δx_{21}	Δy_2	Δz_{21}	Δx_{22}	Δz_{22}	Δ_{31}	Δz_{32}	Mean r factor
SICM33 (best)	−0.65	−0.30	0.045	0.75	0.445	−0.06	−0.10	0.136	0.12	0.136	−0.152	0.208	0.174 (θ=0°) 0.150 (θ=15°, ϕ=135°)
SICM35	−0.65		0.045	0.75	0.445	−0.06		0.136	0.12	0.136	−0.152	0.208	0.212 (θ=0°)
YC[a]	−0.573		0.159	1.038	0.468	−0.093		0.047	0.115	−0.020	−0.139	0.185	0.258 (θ=0°)
Ch[b]	−0.478		−0.100	1.071	0.459	−0.094		−0.075	0.094	0.011	−0.132	0.106	0.364 (θ=0°)

[a]Yin-Cohen model (Ref. 26) modified to eliminate distortions in the fourth layer but *including* x shifts in the third layer (not shown in Fig. 4) and slight dilation of the interlayer spacing between third and fourth atomic layer.

[b]Chadi model (Refs. 27 and 28) modified to limit the distortion to three layers but *including* x shifts in the third layer (not shown in Fig. 4) and slight compression of the interlayer spacing between third and fourth atomic layer.

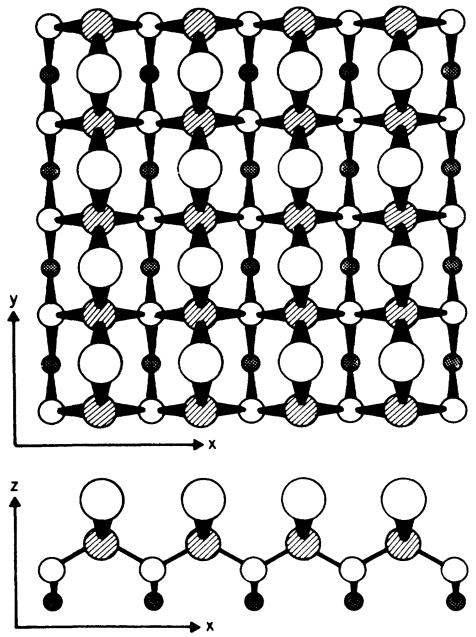

FIG. 5. Schematic representation of undistorted, bulklike Si{001} with perspective view of bonds. Large open circles are atoms in the first layer; shaded circles are atoms in the second layer; small open circles are atoms in the third layer, and small dotted circles are atoms in the fourth layer.

are scarce in the literature and limited to general cases.[25] Hence a detailed discussion of the Si{001} case may be of interest here.

We recall in Fig. 5 the structure of a {001} plane of the Si structure. Although the top atomic layer (largest open circles in Fig. 5) fits in a square net and has, therefore, by itself, fourfold symmetry, the zig-zag characteristics of the back bonds limit the overall symmetry to twofold. Moreover, we see that by "peeling off" the top atomic layer, as may occur, e.g., at a monatomic step, we create another domain (called *B*) related to the first (called *A*) by a 90° rotation around the surface normal. Thus a bulklike Si{001} with monatomic steps would exhibit two types of domains. Equal concentrations of both types would restore fourfold symmetry to the corresponding LEED pattern.

In Fig. 6 we show schematically, on top, two unit meshes of the *A* and two of the *B* bulklike termination, the circles representing atoms in the first atomic layer. In the same figure, *SA* and *SB* represent one unit mesh of 2×1 and 1×2 distortions, respectively, with *symmetric* dimers—there are still only two domains. If we allow asymmetric and buckled dimers, however, arising from atomic shifts along both edges of the unit mesh and perpendicular to the surface, we get four possible domains on the *A* surface (denoted 1*A*,2*A*,3*A*,4*A* in Fig. 6, the larger circle representing the atom that moves up) and four on the *B* surface (1*B*,2*B*,3*B*,4*B*). In principle, therefore, we should carry out eight intensity calculations, one for each domain, and then average them according to some reasonable assumption about the concentration of each type of domain on the surface (in the absence of specific informa-

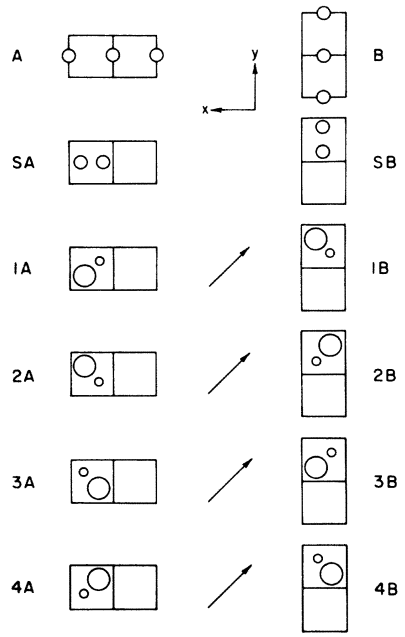

FIG. 6. A and B represent two unit meshes of bulklike undistorted Si{001}, the circles representing top-layer atoms. SA and SB represent symmetric dimer distortions of A and B, respectively. $1A$, $2A$, . . . , $4B$ represent the eight equivalent domains possible on the A and B surfaces, respectively, for asymmetric and buckled dimers (larger circles represent the atom moving up). The arrows represent $\vec{k}_{par}$ in the experiment at non-normal incidence.

tion we assume equal concentrations). However, if we examine the symmetry relationships between domains we see that we can reduce the number of intensity calculations considerably. At normal incidence we need only one such calculation; at non-normal incidence, if we select an appropriate azimuth, we need four intensity calculations. We explain the procedure in the following.

At normal incidence, when the component $\vec{k}_{par}$ of the incident wave vector parallel to the surface plane vanishes, there are simple relationships among domains. We see in Fig. 6 that from $1A$ we get to $1B$ by a 90° clockwise rotation, and to $2A$ by reflection around a horizontal mirror plane. The complete relationship is summarized as follows:

$$1A \xrightarrow{90^\circ\text{ rot}} 1B \xrightarrow{90^\circ\text{ rot}} 4A \xrightarrow{90^\circ\text{ rot}} 4B ,$$

$$\downarrow$$

horizontal mirror

$$\downarrow$$

$$2A \xrightarrow{90^\circ\text{ rot}} 2B \xrightarrow{90^\circ\text{ rot}} 3A \xrightarrow{90^\circ\text{ rot}} 3B .$$

Consider, for example, the experimental 1 0 beam. If all eight domains are equally represented on the surface, this beam is the average of the 1 0 beams from each domain,

$$(1\,0)_{expt}=[(1\,0)_{1A}+(1\,0)_{2A}+(1\,0)_{3A}+(1\,0)_{4A}+(1\,0)_{1B}+(1\,0)_{2B}+(1\,0)_{3B}+(1\,0)_{4B}]/8 .$$

But the symmetry relationships listed above require that

$$(1\,0)_{2A}=(1\,0)_{1A},\quad (1\,0)_{3A}=(\bar{1}\,0)_{1A} ,$$

$$(1\,0)_{4A}=(\bar{1}\,0)_{1A},\quad (1\,0)_{1B}=(0\,1)_{1A} ,$$

$$(1\,0)_{2B}=(0\,\bar{1})_{1A},\quad (1\,0)_{3B}=(0\,1)_{1A} ,$$

$$(1\,0)_{4B}=(0\,\bar{1})_{1A} ,$$

hence

$$(1\,0)_{expt}=[(1\,0)_{1A}+(\bar{1}\,0)_{1A}+(0\,1)_{1A}+(0\,\bar{1})_{1A}]/4 .$$

Thus we only need calculate the intensities of the beams produced by the $1A$ domain and then average them according to the general rule:

$$(I_{hk})_{expt}=(I_{hk}+I_{\bar{h}k}+I_{h\bar{k}}+I_{\bar{h}\bar{k}}+I_{kh}+I_{\bar{k}h}+I_{k\bar{h}}+J_{\bar{k}\bar{h}})/8 ,$$

where the subscript $1A$ on the right-hand side has been dropped. The rule applies to both integral- and fractional-order beams, with the understanding that if the $1A$ domain has a 2×1 (as opposed to a 1×2) super structure, then only the first index can be fractional (i.e., there are no $0\,\frac{1}{2}$, $0\,\frac{3}{2}$, $1\,\frac{1}{2}$, etc., beams).

At non-normal incidence, if the azimuth angle has general (as opposed to special) values, there are no relations between domains because any symmetry operations involve and hence change $\vec{k}_{par}$ as well. In these cases each domain requires a separate intensity calculation: In the present case, eight calculations would be needed. However, if the orientation of $\vec{k}_{par}$ is chosen in such a way that $\vec{k}_{par}$ is unaffected by the symmetry operation relating the domains to one another, then the number of intensity calculations can be reduced. If $\vec{k}_{par}$ is oriented at 135° from the x axis, as indicated by the arrows in the middle of Fig. 6, then by mirroring across $\vec{k}_{par}$ we can bring into coincidence four pairs of domains:

$$1A \leftrightarrow 3B ,$$

$$2A \leftrightarrow 4B ,$$

$$3A \leftrightarrow 1B ,$$

$$4A \leftrightarrow 2B .$$

Thus if we calculate the beam intensities produced by domain $1A$, we know those produced by domain $3B$ as well, because as we can see from Fig. 7,

$$(1\,0)_{3B}=(0\,\bar{1})_{1A},\quad (0\,1)_{3B}=(\bar{1}\,0)_{1A} ,$$

$$(0\,\tfrac{1}{2})_{3B}=(\bar{\tfrac{1}{2}}\,0)_{1A} ,$$

etc. If the indexing of the experimental beams was, e.g., the one depicted in Fig. 7 for domain $1A$, then the contributions to, e.g., the experimental 1 0 beam will be the 1 0 beam of $1A$ and the 1 0 beam of $3B$, or

$$(1\,0)_{expt}\propto(1\,0)_{1A}+(1\,0)_{3B}=(1\,0)_{1A}+(0\,\bar{1})_{1A} .$$

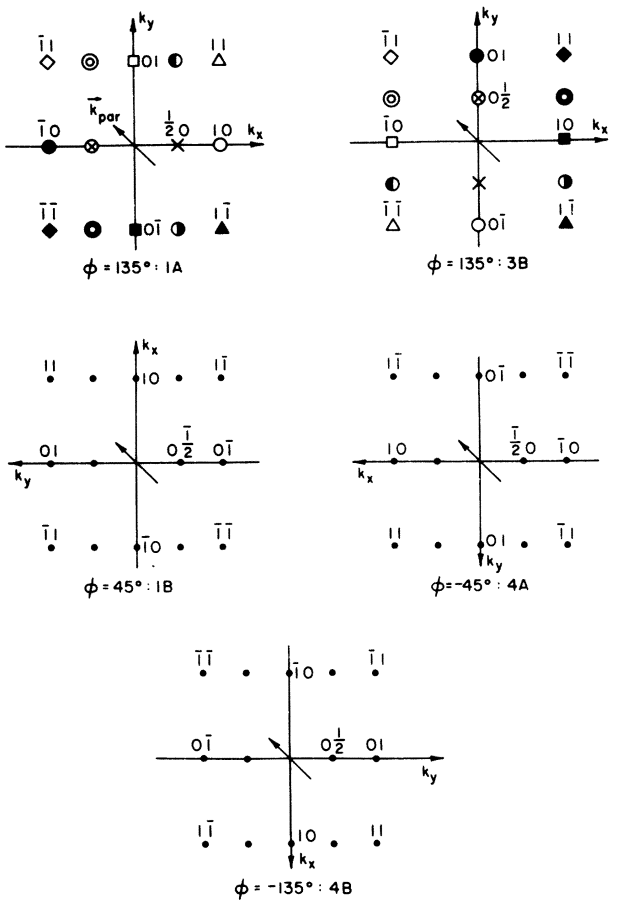

FIG. 7. Two top drawings represent schematically LEED patterns at non-normal incidence and $\phi = 135°$ for the $1A$ (left) and the $3B$ (right) domains. Figure 6 defines the domains. The LEED spots are drawn with different symbols to facilitate recognition of the symmetry relation between $1A$ and $3B$ domains: mirroring across $\vec{k}_{par}$ (inclined arrow). The three lower drawings are schematic LEED patterns, with beam indices, for domains $1B$ at $\phi = 45°$, $4A$ at $\phi = -45°$, and $4B$ at $\phi = -135°$ (see text).

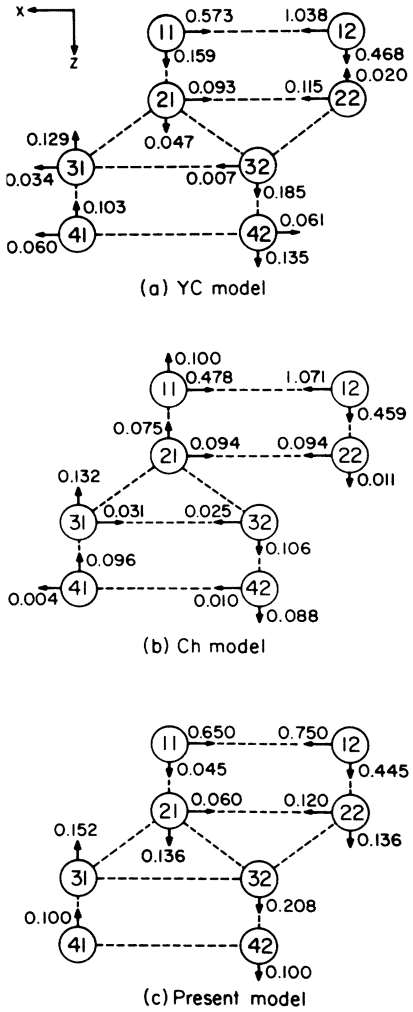

FIG. 8. Schematic side views of Si{001} with arrows and numbers indicating direction and magnitude of atomic shifts in three models: (a) YC (Ref. 27); (b) Ch (Ref. 9); (c) this work. Note that this view does not show the y shifts present in (c) and depicted in Fig. 4.

In general, $(I_{hk})_{expt} \propto I_{hk} + I_{\bar{h}\bar{k}}$. This process is referred to as "internal averaging" because it consists of averaging beam intensities within a single calculation for one domain. Similar internal averaging rules are derived from the above symmetry relationships. It is obvious, therefore, that we need do only four intensity calculations, for example, one each for domains $1A$, $2A$, $3A$, $4A$, or the domains $1A$, $4B$, $1B$, $4A$, etc., and then apply the appropriate internal-averaging procedures.

One more comment about the four intensity calculations may be useful. The most direct way to proceed is to set up the atomic coordinates for domain $1A$ in a suitable coordinate system, fixing the value of the azimuth ϕ (for a precise definition of ϕ see, e.g., Jona[18]) and then calculate the LEED beam intensities with the CHANGE program (or equivalent). Then we could change all atomic coordinates, keeping coordinate system and ϕ constant, to represent domain $2A$ and repeat the intensity calculation, and so on for $3A$ and $4A$. This way is, however, beset with the danger of errors in the process of entering anew all the values of the atomic coordinates for each calculation. A less dangerous way is to keep the atomic coordinates as chosen for domain $1A$ but rotate the coordinate system, i.e., simply change the value of the azimuth ϕ. We can arrive at domain $1B$ by rotating domain $1A$ *with* the coordinate system 90° clockwise (Fig. 6), which is equivalent to rotating the reciprocal net 90° counterclockwise (Fig. 7). Hence since $\phi = 135°$ for $1A$, then $\phi = 45°$ for $1B$. Similarly, $\phi = -45°$ for $4A$ and $\phi = -135°$ for $4B$. The final-averaging rules are also obvious from Fig. 7: For example, assuming again that the indexing of the experimental beams follows that chosen for domain $1A$,

$$(1\,0)_{expt} \propto (1\,0)_{1A} + (0\,\bar{1})_{1B} + (\bar{1}\,0)_{4A} + (0\,1)_{4B} ,$$

and finally, including the internal averaging as discussed above,

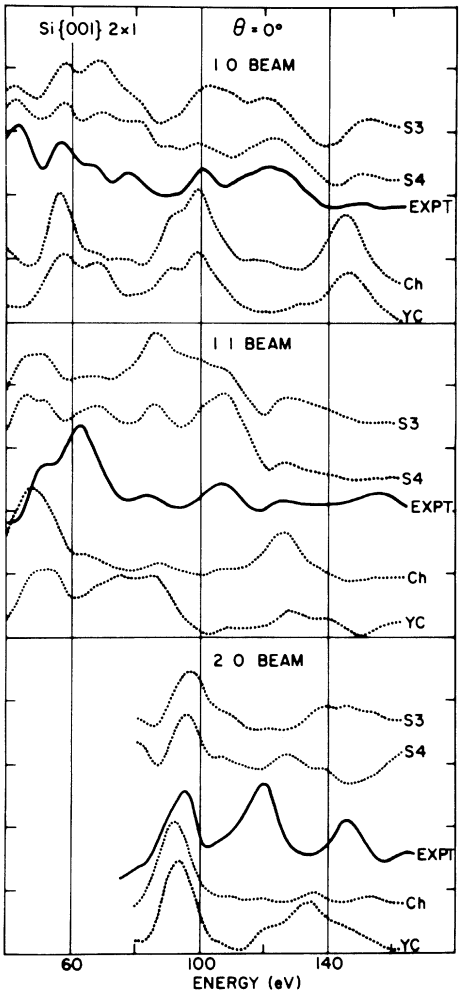

FIG. 9. LEED test at normal incidence (integral-order beams) for four models. YC, Yin and Cohen (Ref. 26); Ch, Chadi (Refs. 27 and 28); *S*3 and *S*4, three- (SICM33) and four-layer-distorted model reported here; EXPT, experimental data SB(NI) (see Fig. 1).

$$(10)_{\text{expt}}=(10+0\bar{1})_{1A}+(0\bar{1}+\bar{1}0)_{1B}$$
$$+(\bar{1}0+01)_{4A}+(01+10)_{4B}\ .$$

IV. TESTS OF THEORETICAL MODELS, RESULTS, AND DISCUSSION

It was mentioned in Sec. I that while there seems to be general agreement on the type of model that describes the 2×1 reconstruction of Si{001}, namely, the asymmetric and buckled dimer model, and various specific quantitative geometries have been proposed in this regard, there is no general agreement on precisely which atomic arrangement is correct. Yin and Cohen[26] (YC) developed an energy-minimization scheme for the determination of surface atomic geometries by calculating total energies of slabs with an *ab initio* self-consistent local-density pseudopotential procedure. They applied this scheme to Si{001}2×1 and produced a specific model involving distortions in four layers, which is depicted in Fig. 8. Chadi (Ch) also calculated total energy but used a semi-

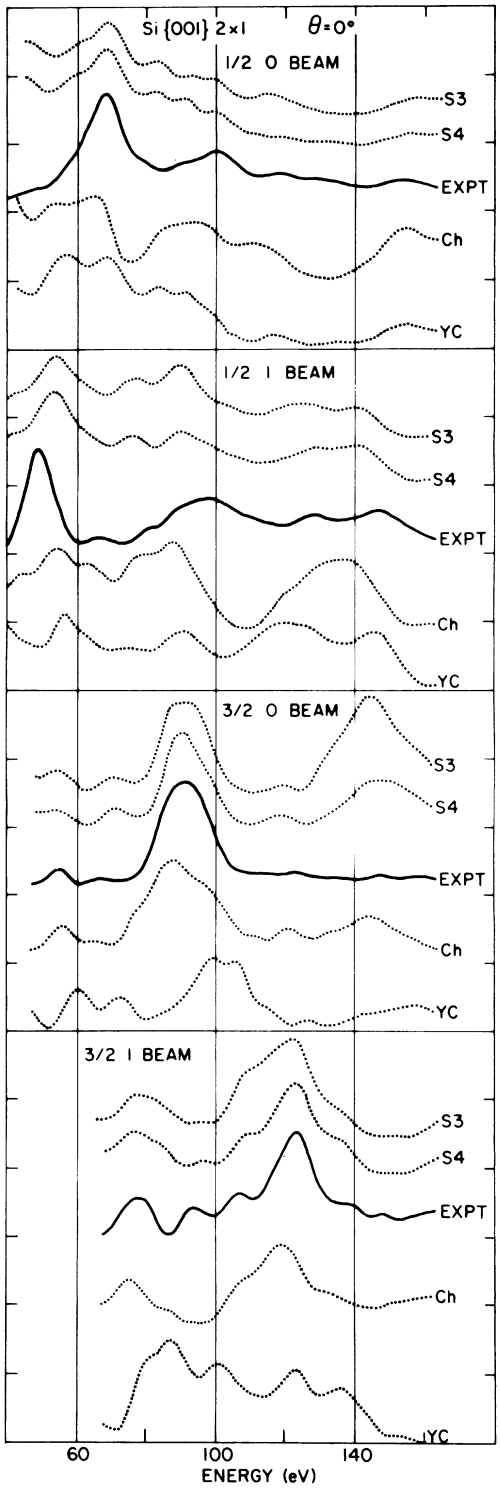

FIG. 10. LEED test at normal incidence (fractional-order beams) for four models. YC, Yin and Cohen (Ref. 26); Ch, Chadi (Refs. 27 and 28); *S*3 and *S*4, three- (SICM33) and four-layer-distorted model reported here; EXPT, experimental data SB(NI) (see Fig. 1).

empirical approach to estimate the contributions of ion-ion and electron-electron interactions.[27] He later minimized the total energy to generate a quantitative model for Si{001}2×1 with distortions involving eight atomic

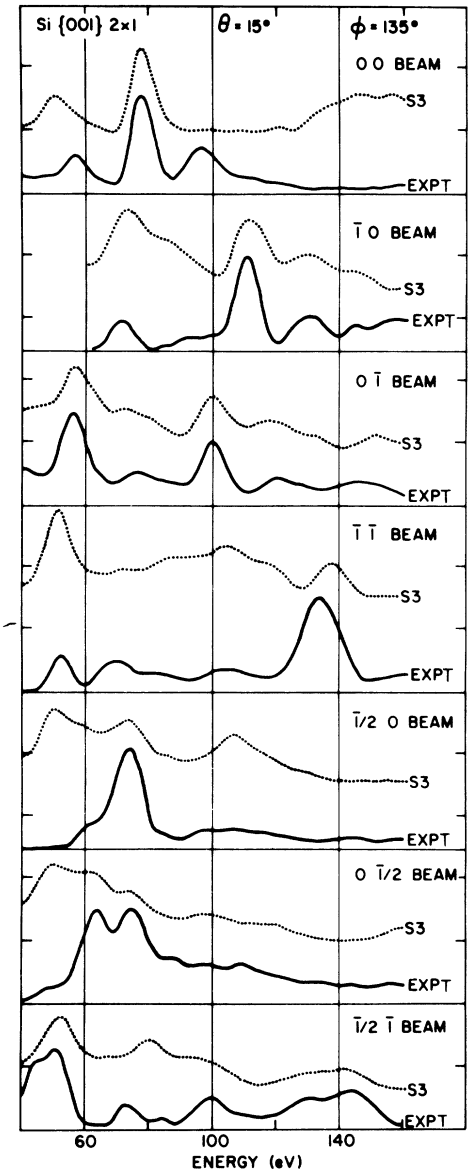

FIG. 11. LEED test at $\theta=15°,\phi=135°$. *S*3, three-layer-distorted model (SICM33); EXPT, experimental data SB(PT) (see Fig. 2).

layers.[28] We present in Fig. 8 a four-layer distorted version of Chadi's model that can be compared to both YC's and our own model. (But note that our model involves atomic shifts in the y direction which the other two models do not have.) As we can see from Fig. 8, there are marked differences between the three models. The LEED test provides a quantitative means of evaluating them and discriminating against incorrect models. To pass the LEED test, the LEED spectra calculated with a FD program for a given model must agree well the experimental LEED spectra. There is no established rule about *how well* a model must pass the LEED test before it can be labeled as essentially correct. But we know that a model which fails the LEED test must be wrong. In practice, even if a model does pass the LEED test adequately as fixed by standards built up by experience, we still cannot be sure that no other model would pass the LEED test better. However, the probability of such a better model existing is small, particularly if the structure is complicated and the data base for the analysis is large.

We have subjected both the YC and the Ch model to the LEED test at normal incidence and we present the results in Figs. 9 and 10. To be sure, the models that we have tested are only three-layer-distorted versions of the YC and Ch model, as described in Table I, but we know from experience that while the contribution of the fourth layer may in some cases be noticeable, it can never convert a model from nonacceptable to acceptable. We see from the figures that there are serious discrepancies between the calculated and the observed LEED spectra for both models—it is fair to say that neither the YC nor the Ch model passes the LEED test. The mean r-factor values are quoted in Table I. The poor showing of these models at normal incidence does not justify our proceeding with the costly and elaborate analysis at non-normal incidence. We can see from Figs. 9 and 10 that the model labeled SICM33 in Table I passes the LEED test adequately. The agreement between theory and experiment is encouraging enough, in fact, to justify a calculation for the same model *plus* a distortion in the fourth layer, as depicted in Fig. 8(c). The LEED spectra calculated for this model are also shown in Figs. 9 and 10, and agree with experiment better than the spectra from the three-layer-distorted model. However, the test at non-normal incidence ($\theta=15°$, $\phi=135°$) was carried out only for the latter model (SICM33). Figure 11 shows all seven spectra used in the test. We note again that the agreement between theory and experiment, while not excellent, is remarkably good

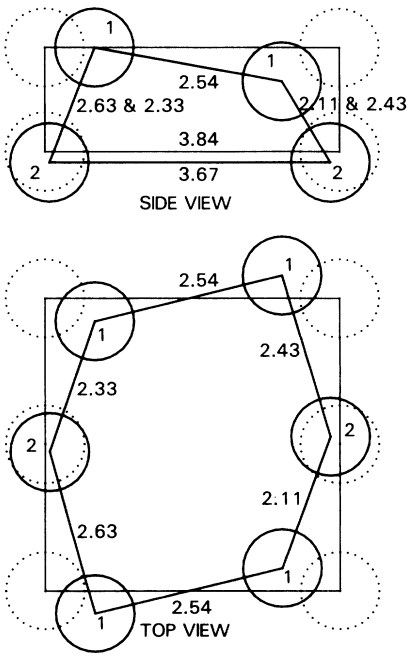

FIG. 12. Atom positions in the first two layers showing side and top views of the structure from LEED analysis. Dotted circles are truncated bulk positions, solid circles are reconstructed positions. First-layer atoms are labeled 1, second-layer atoms are labeled 2. True lengths are given in Å although some bonds are seen in projection.

TABLE II. Atom movements in Si{001}2×1 structure models. The coordinates of atoms 11, 12, 21, and 22 (see Fig. 4) are denoted as $x_{11}, y_{11}, z_{11}, x_{12}, y_{12}, z_{12}, \ldots$, and their shifts from bulk positions as $\Delta x_{11}, \Delta y_{11}, \Delta z_{11}, \ldots$. The dimer bond d_1, the average relaxation of first-layer spacing d_2, the buckling of the first layer d_3, and the y-asymmetry d_4 are defined as follows (values in Å): $d_1 = [(x_{12}-x_{11})^2 + (y_{12}-y_{11})^2 + (z_{12}-z_{11})^2]^{1/2}$, the percent change is $100(d_1-2.35)/2.35$, $d_2 = (\Delta z_{11} + \Delta z_{12})/2 - (\Delta z_{21} + \Delta z_{22})/2$, the percent change is $100d_2/1.36$, $d_3 = |\Delta z_{11} - \Delta z_{12}|$, the percent change is $100d_3/1.36$, $d_4 = |\Delta y_{11} - \Delta y_{12}|$, the percent change is $100d_4/3.84$.

Model	d_1 (Dimer bond) Å	%	d_2 (Layer relaxation) Å	%	d_3 (Buckling first layer) Å	%	d_4 (y asymmetry) Å	%
LEED (present work)	2.54	8.1	0.109	−8.0	0.40	29	0.60	16
Appelbaum and Hamann (Ref. 2)	2.44	3.8	0.114	−8.4	0.0	0	0.0	0
Yin and Cohen (Ref. 26)	2.25	−4.3	0.30	−22.0	0.31	23	0.0	0
Chadi (Ref. 28)	2.35	0.0	0.21	−15.6	0.56	41	0.0	0
Verwoerd (Ref. 29)	2.46	4.7	0.25	−18.0	0.48	35	0.0	0

for a structure as complicated as this one. It is possible that the assumption of equal representation of all domains on the surface was not quite correct, and it is almost certain that the values of the structural parameters are not yet optimized. However, the quality of agreement and the low r-factor values quoted in Table I have never been attained before on this structure and indeed correspond to highly reliable structures in many other systems. Thus we must conclude that the model labeled SICM33 in Table I and indeed its extension to four layers as depicted in Fig. 8(c) pass the LEED test satisfactorily.

It is difficult to estimate the reliability of each single structural parameter in the model. In general, the z coordinates (perpendicular to the surface) are believed to be more accurate than the x and y coordinates, because at and near normal incidence the LEED spectra are more sensitive to z shifts than to others. Our experience with Si{001}2×1 suggests that each atomic parameter listed in Table I is very probably within about 0.1 Å from its "correct" value, although for some parameters (like the z shifts) the margins may be narrowed perhaps to 0.05 Å. We would like to emphasize the fact that, at this stage, the model presented here is *as a whole* the best available to date and the one that gets closest to represent the structure of reconstructed Si{001}2×1. Whether any specific parameter can be further refined, which one and to what extent, are open questions. A study of the sensitivity of LEED analysis to the 12 structural parameters defined in Table I can be done, but by present methods would be very costly and time consuming.

As pointed out in our short Communication,[11] the most novel attribute of our model, beyond the fact that it produces the best agreement with experiment to date, is the fact that it involves atomic shifts in the y direction (see Fig. 4 and Table I). We have made only one test of the importance of this particular parameter, namely, the calculation labeled SICM35 in Table I for a model without the y shifts but otherwise identical to SICM33. The mean r factor is about 20% larger for SICM35 than for SICM33. Whether a special combination of the other 11 structural parameters exists that would produce an even lower r factor *without* involving y shifts, we do not know—we did not find it.

Figure 12 is a scaled drawing of the actual atomic positions in the first two layers of our model as projected on the {010} and {001} planes. We see that the dimer length is 2.54 Å (8% larger than bulk). The only other experimental determination of this parameter that we are aware of is due to Aono *et al.*,[10] who used low-energy ion scattering in a special geometry to determine the "intradimer atomic distance parallel to the surface" as 2.4±0.1 Å, in fair agreement, within the combined estimated errors, with our value. The corresponding values in the theoretical models are 2.25 Å (YC[27]), 2.35 Å (Ch[29]), and 2.46 Å (Verwoerd[29]) (see Table II). We also note that our model has a much smaller average contraction of the first interlayer spacing with respect to the bulk (8%) than any of the theoretical models (22% for YC, 16% for Ch, and 18% for Verwoerd). The Si—Si bonds in our model are all within 4% of the bulk value with two exceptions: the bond between atoms 11 and 21 (see Fig. 4), at 2.63 Å 12% larger than the bulk value, and the bond between atoms 12 and 22, at 2.11 Å 10% smaller than the bulk value.

ACKNOWLEDGMENT

Two of the authors (W.S.Y. and F.J.) are grateful to the National Science Foundation for partial support of this work.

*Present address: Department of Physics, University of Peking, Peking, People's Republic of China.

[1]J. A. Appelbaum, G. A. Baraff, and D. R. Hamann, Phys. Rev. Lett. 35, 729 (1975); Phys. Rev. B 15, 2408 (1977).

[2]J. A. Appelbaum and D. R. Hamann, Surf. Sci. 74, 21 (1978).

[3]S. Y. Tong and A. L. Maldonado, Surf. Sci. 78, 459 (1978).

[4]F. Jona, H. D. Shih, D. W. Jepsen, and P. M. Marcus, J. Phys. C 12, L455 (1979).

[5]S. J. White, D. C. Frost, and K. A. R. Mitchell, Solid State Commun. 42, 763 (1982).

[6]J. E. Rowe and H. Ibach, Phys. Rev. Lett. 32, 421 (1974).

[7]F. J. Himpsel and D. E. Eastman, J. Vac. Sci. Technol. 16,

1297 (1979); Phys. Rev. Lett. 45, 1112 (1980).
[8]M. J. Cardillo and G. E. Becker, Phys. Rev. Lett. 40, 1148 (1978).
[9]R. M. Tromp, R. G. Smeenk, and F. W. Saris, Solid State Commun. 39, 755 (1981).
[10]M. Aono, Y. Hou, C. Oshima, and Y. Ishizawa, Phys. Rev. Lett. 49, 567 (1982).
[11]W. S. Yang, F. Jona, and P. M. Marcus, Solid State Commun. 43, 847 (1982).
[12]P. M. Marcus and F. Jona, Appl. Surf. Sci. 11/12, 20 (1982).
[13]A. Ignatiev, F. Jona, M. Debe, D. E. Johnson, S. J. White, and D. P. Woodruff, J. Phys. C 10, 1109 (1977).
[14]J. J. Lander and J. Morrison, J. Appl. Phys. 33, 2089 (1962); J. Chem. Phys. 37, 729 (1962).
[15]T. D. Poppendick, T. C. Ngoc, and M. B. Webb, Surf. Sci. 75, 287 (1978).
[16]K. Mueller, E. Land, L. Hammer, W. Grimm, P. Heilmann, and K. Heinz, Proceedings of the Conference on Determination of Surface Structures by LEED, Yorktown Heights, 1980 (unpublished).
[17]The first detailed comparison of LEED spectra for the same surface from different sources was done by M. G. Lagally [Z. Naturforsch. A 25, 1567 (1980)] for Ag{111}. The data were collected with a Faraday cage and were limited to the 0 0 spectrum. However, the curves used for that comparison no longer reflect the state of the art in LEED experimentation. An international "LEED Clean Surface Intensity Project" is currently underway for Cu{001} but no results will be available for some time.
[18]F. Jona, J. Phys. C 11, 4271 (1978).
[19]J. C. Fernandez, W. S. Yang, H. D. Shih, F. Jona, D. W. Jepsen, and P. M. Marcus, J. Phys. C 14, L55 (1981).
[20]S. Y. Tong, M. A. van Hove, and B. J. Mrstik, in *Proceedings of the Seventh International Vacuum Congress and the Third International Conference on Solid Surfaces, Vienna, 1977,* edited by R. Dobrozemsky *et al.* (Berger, Vienna, 1977), Vol. 3, p. 2407.
[21]D. W. Jepsen, H. D. Shih, F. Jona, and P. M. Marcus, Phys. Rev. B 22, 814 (1980).
[22]F. Jona, H. D. Shih, D. W. Jepsen, and P. M. Marcus, J. Phys. C 12, L455 (1979).
[23]E. Zanazzi and F. Jona, Surf. Sci. 62, 61 (1977).
[24]Mathematical Statistics Group of the Institute of Mathematics, *Orthogonal Experimental Methods* (Academy of Sciences of the People's Republic of China, 1975) (in Chinese).
[25]See, e.g., J. B. Pendry, *Low Energy Electron Diffraction* (Academic, New York, 1974), p. 228ff; F. Jona, J. Phys. C 11, 4271 (1978); F. Jona, J. A. Strozier, Jr., and W. S. Yang, Rep. Prog. Phys. 45, 527 (1982).
[26]M. T. Yin and M. L. Cohen, Phys. Rev. B 24, 2303 (1981).
[27]D. J. Chadi, Phys. Rev. Lett. 41, 1062 (1978); Phys. Rev. B 19, 2074 (1979); Phys. Rev. Lett. 43, 43 (1979).
[28]D. J. Chadi (unpublished).
[29]W. S. Verwoerd, Surf. Sci. 103, 1104 (1981).